Article

Journal of
Nanoscience and Nanotechnology
Vol. 19, 2027–2033, 2019
www.aspbs.com/jnn

Copyright © 2019 American Scientific Publishers
All rights reserved
Printed in the United States of America

Hemoglobin Immobilization on Multiporous Nanofibers of SnO_2 and Chitosan Composite for Hydrogen Peroxide Sensing

A. K. M. Kafi*, Samiul Alim, Rajan Jose, and Mashitah M. Yusoff

Faculty of Industrial Sciences and Technology, Universiti Malaysia Pahang, Kuantan 26300, Malaysia

A multiporous nanofiber (MPNFs) of SnO_2 and chitosan has been used for the immobilization of a redox protein, hemoglobin (Hb), onto the surface of glassy carbon electrode (GCE). The multiporous nanofiber of SnO_2 that has very high surface area is synthesized by using electrospinning technique through controlling the tin precursor concentration. Since the constructed MPNFs of SnO_2 exposes very high surface area, it increases the efficiency for biomolecule-loading. The morphology of fabricated electrodes is examined by SEM observation and the absorbance spectra of Hb/(MPNFs) of SnO_2 are studied by UV-Vis analysis. Cyclic Voltammetry and amperometry are employed to study and optimize the performance of the resulting fabricated electrode. After fabrication of the electrode with the Hb and MPNFs of SnO_2, a direct electron transfer between the protein's redox centre and the glassy carbon electrode was established. The modified electrode has showed a couple of redox peak located at -0.29 V and -0.18 V and found to be sensitive to H_2O_2. The fabricated electrode also exhibited an excellent electrocatalytic activity towards the reduction of H_2O_2. The catalysis currents increased linearly to the H_2O_2 concentration in a wide range of 5.0×10^{-6}–1.5×10^{-4} M. Overall experimental results show that MPNFs of SnO_2 has a role towards the enhancement of the electroactivity of Hb at the electrode surface. Thus the MPNFs of SnO_2 is a very promising candidate for future biosensor applications.

Keywords: Multiporous SnO_2 Nanofiber, Hemoglobin, Direct Electrochemistry, Electrical Contact, H_2O_2 Sensing.

1. INTRODUCTION

Since early 1970's, scientists start to couple an enzyme with an electrochemical sensors in order to establish the concept of biosensors.[1] The key over other types of are including ability of fast and rapid response, ease of preparation, low cost, very small amount of reagents required for calibration and ability to measure non-polar molecules.[2,3] In order to construct an electrochemical sensitive biosensor, the biological recognition materials must be in intimate contact with the transducer. Redox enzyme/proteins are the most widely used biomolecules to study and configure the electrochemical biosensor.[4,5] The execution of a biosensor primarily relies on upon the properties of the immobilized biomolecules connected with the transducer. A major challenge in biosensors is the stable immobilization of biomolecules on electrical components with complete retention of their biological recognition properties.[6,7] Various traditional types of immobilization techniques such as cross-linking, covalent binding and entrapment in gels or membranes show a low reproducibility and a poor spatially controlled deposition.[8,9] Additionally, other notable challenges for designing biosensors are including implementing biocompatible materials that do not kill biomolecules and maintain the native structure, while not compromising device operation. Special properties of redox enzymes/proteins, which catalyze the oxidation or reduction reactions, are extremely useful while being used in designing electrochemical biosensors.[10–13]

Hemoglobin (Hb) which is the important component of red blood cells (RBC). It is one kind of protein that transports the oxygen (O_2) from the lungs and carries O_2 to body tissues. It has an approximated 67,000 $gmol^{-1}$ molar

*Author to whom correspondence should be addressed.

mass which considers as large protein.[14] Hb has been used as a favorable biomolecules for the development of hydrogen peroxide (H_2O_2) biosensor based on the direct electron transfer (DET) reaction because it has four electroactive iron heme.[15] A critical challenge of any biosensors is to develop excellent communication between the biosensing elements (e.g., enzyme, redox protein) and the transducers (electrode).[16–20] Hemoglobin, a large redox protein will cause blocking of electron to transfer by irreversibly adsorbed on the bare electrode surface.[21,22] Thus, in order to improve the electron transfer reaction, special modified layer on the bare electrode surface or use of mediators have been reported.[19,23–25] And those results revealed that the adding a further layer improved biosensor performances. In this regards, over the past two decades, various methods, such as embedding enzymes in conductive polymer films, diffusional electron mediators, functionalization of the enzymes with redox-relay units are common methods to establish electron-transfer communication between the redox sites in the enzymes and the electrodes.[26–31] However, major drawbacks inherent to the enzyme-based sensors include the difficulty in enzyme immobilization and their limited lifetime due to desorption and deactivation of the immobilized enzymes.[32] In this context, for a researcher, a probe with a nano-dimensional is enticing in order to precisely sense the target analytes while designing biosensors. Nanobiotechnology is defined as a field of science directed to design materials, devices, and systems possessing certain specified functions and composed of nanoscale elements. In recent years, the applications of nanomaterials in biosensors have also advanced greatly since they possess the unique electrical properties, high chemical stability and high surface-ratio to-volume.[33–35] Several nanostructured materials have not been yet studied well specially in biosensing application due to application diversity. Thus, a lot of novel nanomaterials are being fabricated and their novel properties are being explored which are highly needed.[34,36] For this purpose, sensors with nanoscale dimensions, such as nanotubes or nanowires, have been developed for effective biosensing and diagnostics purposes.[37]

Tin oxide (SnO_2) is a kind of metal oxide which exists in thin film form. Nowadays, nanostructured form of SnO_2 is playing very important role in application of gas sensors, materials of electrode and also in solar cells.[38,39] This is due to its intelligent photo-electronic property, high sensitivity with a shorter response time when compared with other inorganic oxides. Recently, we have fabricated one-dimensional nano-morphologies of SnO_2, named as multiporous nanofibers (MPNFs), via electrospinning by controlling the tin precursor concentration.[40] Fabricated MPNFs possessed the highest surface area with superior charge transport characteristics. These enhanced characteristics of the MPNFs would be excelled in comparison with other conventional nanofibers and nanowires if employed in biosensing. Considering those special characteristics above, we have developed a new electrode modified with SnO_2-MPNFs, Chitosan and Hemoglobin for electrochemical determination of H_2O_2. The proposed composite, SnO_2-MPNFs/chitosan/Hemoglobin could be a potential material for biosensing applications. To the best of our knowledge for the first time, multiporous nanofibers of SnO_2 and chitosan composite has been used to study direct electrochemistry of a redox protein.

2. EXPERIMENTAL DETAILS

2.1. Reagents and Materials

Tin chloride pentahydrate ($SnCl_4 \cdot 5H_2O$), polyvinylpyrrolidone (PVP), dimethylformamide (DMF) were bought from Sigma. Hemoglobin, chitosan and stock solution of 30 wt% H_2O_2, were also purchased from Sigma and used as received and stored at 4 °C. The pure water (18 MΩ · cm) used to prepare all solutions in this work was purified with the Nanopure® water system. All other reagents were of analytical grade. 0.01 M Phosphate buffer solution of pH 7.0 was freshly prepared every time before use. The pH of PBS was adjusted by using 1.0 M hydrochloric acid (HCl) or 1.0 M sodium hydroxide (NaOH) in order to achieve desired pH.

2.2. Fabrication of SnO_2 Nanofiber

In our previous work, we described the fabrication of SnO_2 nanofiber.[40] Briefly, 3 g of PVP was dissolved in an equal volume ratio (1:1) of ethanol and DMF. To this solution, various concentrations of the tin precursor were dissolved at room temperature until the solution became transparent. In brief, the concentrations were 5.5 mM, 7 mM, 8.5 mM, 10 mM, 11.5 mM and were labeled as C0, C1, C2, C3 and C4, respectively. The viscosity of the solution for electrospinning was measured with a rheometer (LVDV III Ultra, Brookeld Co., USA). The solutions were then transferred to a plastic syringe with steel needles for electrospinning, and the operating parameters were as follows: (i) applied voltage, 25 kV, (ii) the injection rate, 0.6 mL h1, (iii) the distance between the collector and the tip of the needle, 20 cm, (iv) humidity, 40–45%, and (v) the speed of the rotating collector, 1200 rpm. Solid nanofibers were then collected from the collector and annealed at temperature 600 C for 3 hour at heating rate 0.5 C min^1.

2.3. Electrode Modification

Fabrication of electrode modified with SnO_2, was executed by following protocol. A glassy carbon electrode (GCE) (3 mm of diameter) has been used to fabricate the electrode. Firstly, the glassy carbon electrode was polished with 0.05 μm alumina slurries successively and was then rinsed with water, acetone, and doubly-distilled water and sonicated. Stock solution of 10 mg of SnO_2 NF was made in 100 μl PBS and the stock solution of 2 mg/ml of Hb

IP: 5.62.157.167 On: Thu, 06 Dec 2018 06:58:07
Copyright: American Scientific Publishers
Delivered by Ingenta

was made in PBS (pH 7.0). Then, 5 μL of SnO_2 NF the stock solution, 5 μL of Hb from the stock solution and 2 μL (2 mg/ml) of chitosan were mixed and dropped on the pre-cleaned GCE surface and allowed to dry for overnight and the modified electrode was rinsed with water prior to measure the electrochemical properties. The final electrode is denoted as SnO_2-NF/Hb/Ch/GCE electrode throughout the paper. We have also fabricated other electrode denoted as Hb/Ch/GCE electrode for a comparison.

2.4. Apparatus and Instrumentation

Scanning electron microscope (SEM) images were captured using a FESEM; JEOLUSA with an accelerating voltage of 100 kV. UV-Vis spectrophotometer, model number of UV-2600 230 V (SHIMADZU) was used to analyze the light absorption of different concentration hemoglobin samples that across wavelength of 350 to 600 nm. All electrochemical measurements were performed with potentiostat PARSTAT 2273. The electrochemical experiments employed a three electrode cell with a SnO_2-NF/Hb/Ch/GCE working electrode, a platinum auxiliary electrode and an Ag/AgCl (sat. KCl solution) reference electrode. Characterization of the modified electrodes was undertaken using cyclic voltammetery (CV) in the windows of potential range −0.8 to +0.2 V. An aqueous solution of 0.01 M phosphate-buffered saline (PBS) pH 7.4 was used as the test electrolyte solution. The buffers were purged with highly purified nitrogen for 30 minutes prior to a series of experiments. A nitrogen environment was kept over solutions in the cell for exclusion of oxygen. All measurements were carried out at room temperature (25 ± 1 °C). A magnetic stirrer was used during electrochemical measurements.

3. RESULTS AND DISCUSSION

3.1. SEM Characterization

Scanning electron microscopy (SEM) was used to characterize the morphologies of the only SnO_2-MPNFs and Hb/SnO_2-MPNFs. A representative scanning electron microscopic image of a multiporous SnO_2 nanofiber is presented in Figure 1(A). As shown in the figure, the obtained SnO_2-MPNFs presented a fibrous structure in all areas with some fiber-fiber interconnections. We have already reported that the MPNFs were formed with grains of size 5–15 nm, which are smaller than the grain size of the PNFs (15–25 nm).[40] And because of the lower grain size and relatively higher polycrystallinity, of MPNFs crystal like structure were observed in MPNFs. And due to the smaller grains, fabricated SnO_2-MPNFs possessed a high surface area. This high surface area of SnO_2-MPNFS allow for a high density proteins/enzyme loading during the design of a biosensor. In Figure 1(B), at the Hb/SnO_2-MPNFs, a network line structure was observed with the aggregation of the immobilized Hb molecules regularly distributed.

(A)
(B)
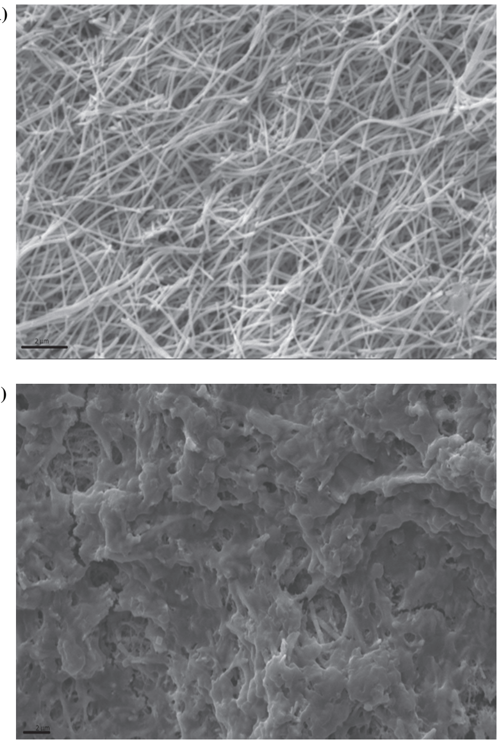

Figure 1. SEM images of (A) multiporous nanofibers of SnO_2, (B) Hb-modified multiporous nanofibers of SnO_2.

IP: 5.62.157.107 On: Thu, 06 Dec 2018 06:58:07
Copyright: American Scientific Publishers
Delivered by Ingenta

The distinguished characters' of the SEM images indicated that Hb existed on the Hb/SnO_2-MPNFs surface.

3.2. UV-Vis Spectroscopy

It is well known that the UV-Vis adsorption spectroscopy is an useful tool to observe the conformation change of heme proteins.[41] In order to investigate the properties of heme of Hb, there were 3 samples used for this spectrophotometry analysis: sample 1 (only hemoglobin), sample 2 (hemoglobin with SnO_2 with the ratio of 1:1), and sample 3 (hemoglobin with SnO_2 and chitosan at the ratio of 2:2:1). Figure 2 shows the UV-Vis spectroscopy results for only Hb (line, a), Hb/SnO_2 (line, b) and Hb/SnO_2/CHIT (line, c). All spectrum results showed the absorbance peak, located at approximate 406 nm, although the absorbance peak was different in height. These results proved that the Hb molecules retained their original conformation in the Hb/SnO_2 and Hb/SnO_2/CHIT solution.

3.3. Electrochemical Measurement of the Modified Electrodes

The electrochemical response of the SnO_2-NF/Hb/Ch/GCE, the Hb/Ch/GCE electrode and a bare glassy carbon electrode was investigated using 0.1 M Phosphate buffer saline (PBS pH 7.0) as an electrolyte media. Figure 3 illustrates a typical cyclic voltammogram of different type of electrodes. We can see that a couple of redox

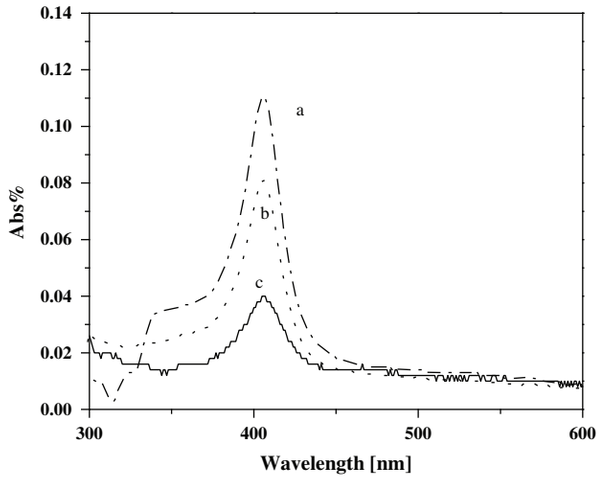

Figure 2. The UV-vis spectroscopy results for Hb (a line), Hb/SnO_2 (b line) and Hb/SnO_2/CHIT (c line).

peaks was shown and it was the representative response of CI.

A redox peak was observed at the GC/Hb/SnO_2/CHIT electrode (curve c) which located at −0.29 V and −0.18 V, cathodic and anodic respectively; in the potential range of from −0.8 V to 0.2 V at a scan rate of 100 mV/s with pH 7.0 PBS. On the other hand, the resulted CV of the Hb/Ch/GCE electrode (curve b) reveals an almost flat respond of the Hb in the same potential range. As expected there was no observable redox peaks attribute to bare glassy carbon electrode. All the results established that Hb created electric communication between the redox centers of itself and the electrodes, as well as SnO_2 played the vital role for direct electron transfer. In addition with this, it can be stated that all the electroactive heme proteins at the GC/Hb/SnO_2/CHIT electrode had been reduced on the forward cathodic scan.[31] The formal potential $E_o = (E_{pa} + E_{pc})/2$ of Hb in GC/Hb/SnO_2/CHIT was calculated

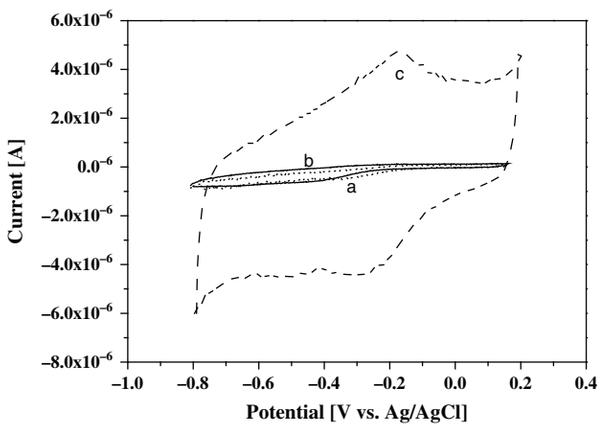

Figure 3. Cyclic voltammograms of the bare GC electrode (curve a), GC/Hb GC/Hb (curve b) and GC/Hb/SnO_2/CHIT electrode (curve c) color line) in 0.01 M PBS (pH 7.0), at a scan rate of 100 mV/s.

to be −0.23 V which was assigned to the heme Fe(III)/Fe(II) transition.[42]

It is already known that the important information involving electrochemical mechanism could be obtained from the relationship between peak current and scan rate.[43] Figure 4(A) shows the electrochemical behaviors of the GC/Hb/SnO_2/CHIT electrode in PBS (pH 7.0) at different scan rates. The peak currents (anodic or cathodic) were linearly dependent on ν at scan rates from 25 to 200 mVs^{-1} in Figure 4(B). This result suggests that the nature of redox process was in the electrode was surface controlled process.[43] This data were further evaluated by creating the relationship between the cathodic peak potential (E_p) and the natural logarithm of a scan rate (ln υ) for the GC/Hb/SnO_2/CHIT electrode. The cathodic peak potential (E_{pc}) changed linearly versus ln ν with a linear regression equation of $Y = -0.04430X - 0.3682$ with $R = 0.9697$, in the range from 50 to 200 mVs^{-1} as shown in Figure 4(C).

Further we calculated the electron-transfer coefficient (α) 0.41, of Hb immobilized at the GC/Hb/SnO_2/CHIT electrode, using the following Eq. (1):[44]

$$E_p = E_o + \frac{RT}{\alpha nF} \ln \frac{RTKs}{\alpha nF} - \frac{RT}{\alpha nF} \ln \upsilon \qquad (1)$$

Here, α is the cathodic electron-transfer coefficient, n is the number of electrons, and T is the temperature; R and F are the gas and Faraday constants, respectively. Then, αn could be calculated to be 0.41. According to a evidenced in the reference, it is usual that $0.3 < \alpha < 0.7$; then, n and α could be concluded to be 1 and 0.41, respectively.[45] From the width of the peak at mid height and a low scan rate, we can also obtain $n = 1$.

IP: 5.62.157.167 On: Thu, 06 Dec 2018 06:58:07
Copyright: American Scientific Publishers
Delivered by Ingenta

3.4. Electrocatalytic Measurement of the Modified Electrodes

Cyclic voltammogram was employed to investigate the response from the electrocatalytic activity of the GC/Hb/SnO_2/CHIT electrode towards the cathodic reduction of hydrogen peroxide. The CVs in the absence and presence of 2.0×10^{-5} M H_2O_2, recorded the GC/Hb/SnO_2/CHIT electrode (Data not shown here). When H_2O_2 was absent in electrolyte (solid line), the GC/Hb/SnO_2/CHIT electrode gives its diffusional redox wave. On the other hand, it is clearly seen that with the addition of hydrogen peroxide, a dramatic cathodic current enhancement was appeared with a simultaneous decrease in the corresponding anodic peak. This indicates that the GC/Hb/SnO_2/CHIT electrode has an excellent electrocatalytic property to H_2O_2 of which was attributed to redox center of Hb.[42] However, it is already reported that the H_2O_2 reduction does not show an obvious catalytic respond at bare glassy carbon electrode.[46] The reaction of redox group of Hb Fe(II) with hydrogen peroxide can be explained with the following equation:

$$HbFe(III) + H_2O_2 \rightarrow \text{Compound I } Fe\{(IV) = O)\} + H_2O \qquad (2)$$

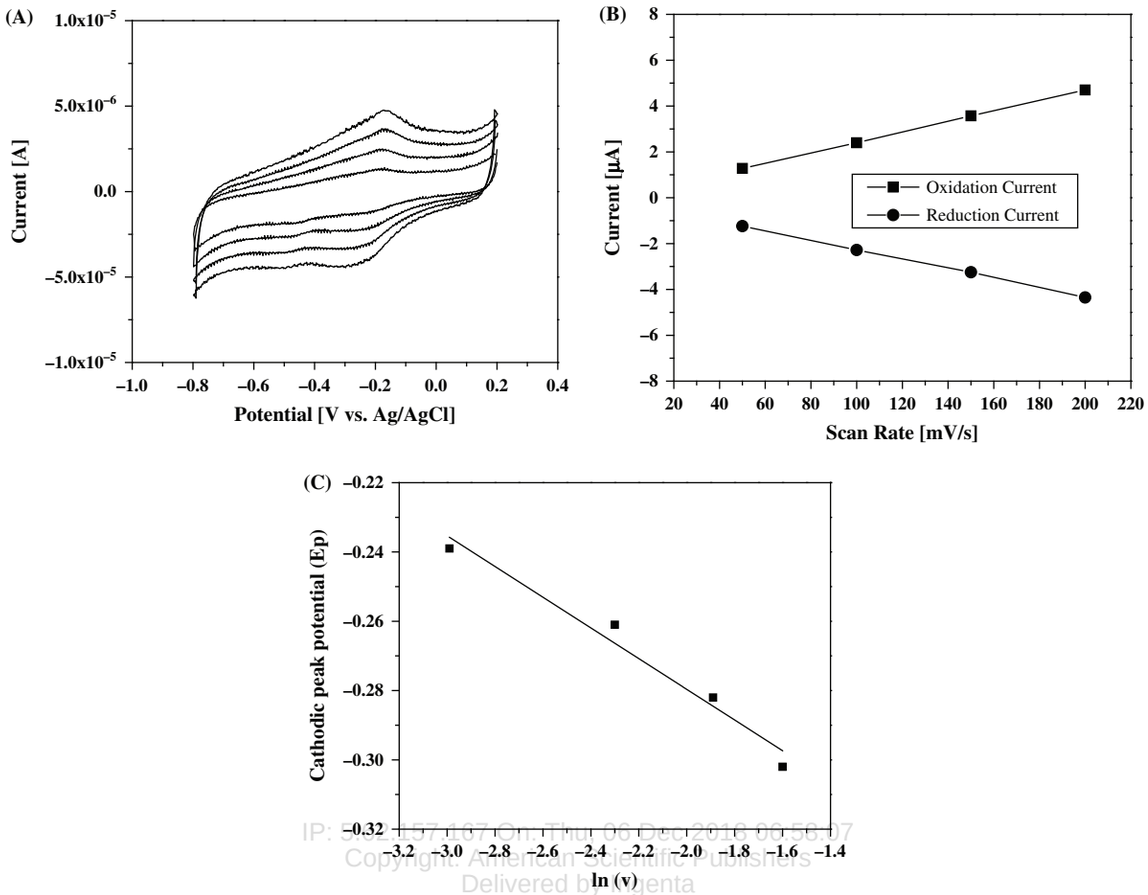

IP: 5[illegible].57.167 On: Thu, 06 Dec 2018 06:58:07
Copyright: American Scientific Publishers
Delivered by Ingenta

Figure 4. (A) Cyclic voltammograms of the GC/Hb/SnO_2/CHIT electrode with various scan rates in 0.1 mol^{-1} PBS with pH 7.0. The scan rates were from 0.05, 0.1, 0.15 and 0.2 V/s from inner to outer way. (B) Reduction and oxidation peak current versus scan rates based on figure (A). (C) The cathodic peak potential versus the logarithm of the scan rate.

$$\text{Compound I } (Fe^{4+}=O) + e^- + H^+ \rightarrow \text{Compound II} \quad (3)$$

$$\text{Compound II } + e^- + H^+ \rightarrow HBFe(III) + H_2O \quad (4)$$

In the presence of H_2O_2 in electrolyte, the oxidation form of the heme group (HbFe(III)) of Hb in the proximity of the electrode is increased, resulting in increased reduction current and the disappearance of the oxidation current.[47]

We have checked the pH dependence of the catalytic current response of the GC/Hb/SnO_2/CHIT electrode in 0.1 M PBS containing 2.0×10^{-5} M hydrogen peroxide. The maximum current response was obtained at pH 7.0, which is close to optimum pH reported for hemoglobin based biosensor. The influence of operating potential on the response of the GC/Hb/SnO_2/CHIT electrode was also investigated. This experiment was accomplished by observing the steady-state current of the GC/Hb/SnO_2/CHIT electrode in the potential range from 0 to −0.5 V in optimal pH 7.0 PBS in the presence of 2.0×10^{-5} M H_2O_2. We found that the steady-state current of catalytic reduction of H_2O_2 on the GC/Hb/SnO_2/CHIT electrode increased gradually as the applied potential shifted from 0 to −0.4 V and then started to decrease slowly as the potential became more negative. Therefore, in order to obtain the highest sensitivity, −0.3 V was selected as the applied potential for the following amperometric measurements.

3.5. Amperometric Response of the Biosensor

The current versus time (i–t) observation of the biosensor was done by successively increasing the H_2O_2 concentration under the optimized conditions in order to further study the performance of the GC/Hb/SnO_2/CHIT electrode. Figure 5 shows the typical amperometry profiles of the GC/Hb/SnO_2/CHIT electrode (curve a) for successive addition of H_2O_2 in a magnetic stirring condition. It is notable that the GC/Hb/SnO_2/CHIT electrode responded immediately to the H_2O_2 increase and achieved 95% of the steady current in 10 s. On the other hand, we can see that much lower response obtained for the GC/Hb/CHIT electrode (curve b) under same experimental conditions. A graph of a calibration curve between amperometric current and H_2O_2 concentration was plotted in Figure 6(A). An acceptable linear relationship for the GC/Hb/SnO_2/CHIT electrode towards H_2O_2 determination, were obtained in the

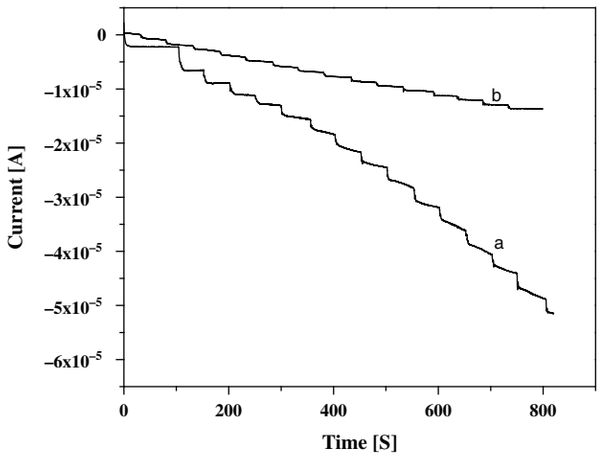

Figure 5. Typical Steady-state amperometric response of the GC/Hb/SnO_2/CHIT electrode (line a) and the GC/Hb/SnO_2/CHIT electrode (line b) with the successive additions of 10×10^{-5} mol l^{-1} H_2O_2 in 0.1 mol l^{-1} PBS (pH 7.0). At the operating potential of −0.3 V.

concentration range from 5.0×10^{-6} to 1.5×10^{-4} M. The limit of detection (LOD) of the biosensor was calculated as the S/N ratio of 3. Where S is the signal and N is the noise. LOD for the biosensor was calculated to be 1.0 μM.

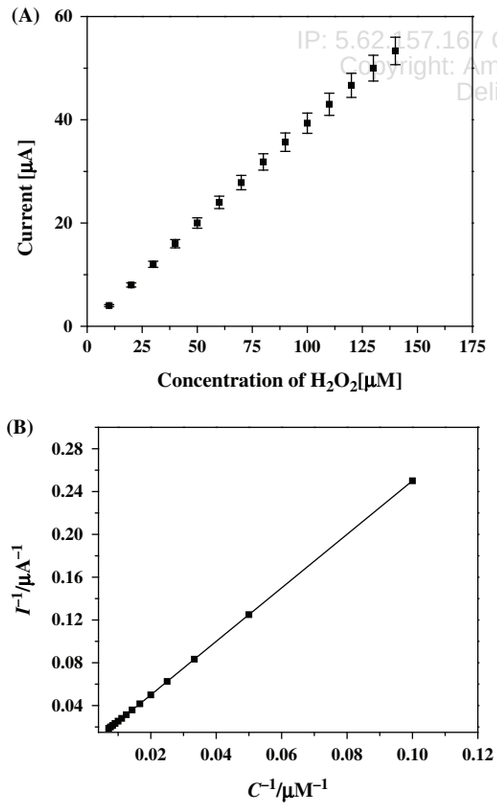

Figure 6. (A) Calibration plot for the the GC/Hb/SnO_2/CH electrode under optimal conditions (calculated based on this Fig. 5). (B) The Lineweaver-Burk plot of $1/I_{ss}$ versus 1/C.

It is known that the K_m (Michaelis-Menten) value gives the indication of the enzyme substrate kinetics for a biosensor which can be obtained using Lineweaver-Burk plot.

$$\frac{1}{i_{ss}} = \frac{K_m^{app}}{i_{max}} \frac{1}{C} + \frac{1}{i_{max}} \quad (5)$$

The K_m value was found to be 0.18 mM using above equation based on Figure 6(B). Relatively a small value of K_m indicates high affinity of Hb toward the H_2O_2, vice versa. This indicated that the proposed electrode exhibited good affinity to H_2O_2.

3.6. Stability, Reproducibility and Repeatability of the Biosensor

The long-term stability of the biosensor is mainly related to the characteristics of protein loading in the SnO_2 nanofiber. The biosensor was stored in 0.1 M PBS (pH 7.0) at 4 °C and the long-term stability of the biosensor was examined by observing the current response of the GC/Hb/SnO_2/CHIT electrode to 2.0×10^{-5} M H_2O_2 by weekly for 35 days. We found that the magnitude of the current response was almost the same as the original value for the first week. However, about 90% initial activity had been retained after 35 days. Excellent stability of this biosensor is presumably because of strong entrapping of Hb into the SnO_2 nanofiber. We fabricated three GC/Hb/SnO_2/CHIT electrodes in same manner in order to verify the reproducibility of the biosensor. All the three GC/Hb/SnO_2/CHIT electrodes were electrochemically characterized by the response of 2.0×10^{-5} M H_2O_2. A relative standard deviation of 4.4% was found, establishing the good reproducibility of the biosensor construction. The repeatability of the biosensor was also assessed by exposing the GC/Hb/SnO_2/CHIT electrode repetitively to a 2.0×10^{-5} M H_2O_2 in PBS (pH 7.0) for ten times. The 5.3% RSD of the response for the biosensor reveals that the biosensor has good repeatability.

IP: 5.62.157.167 On: Thu, 06 Dec 2018 06:58:07
Copyright: American Scientific Publishers
Delivered by Ingenta

4. CONCLUSIONS

In conclusion, the entire work has successfully been done by fabricating a glassy carbon electrode with multiporous SnO_2 nanofiber and hemoglobin to study the direct electrochemistry. Firstly, the morphology of synthesised multiporous SnO_2 nanofiber and Hb modified-multiporous SnO_2 nanofibers were examined by SEM observation. Flowingly, the absorbance spectra of Hb/SnO_2 were studied by UV-Vis analysis revealed that the Hb was still active in multiporous SnO_2 nanofibers surface. Our electrochemical results showed a redox peaks, located at −0.29 V and −0.18 V, which were attributed to the direct electron reaction of hemoglobin in the GC/Hb/SnO_2/CHIT electrode. The formal potential of Hb in fabricated electrode was −0.23 V which was assigned to the heme Fe(III)/Fe(II) transition. After addition of H_2O_2, a clear increase of reduction peak was observed which indicated that Hb

retained its bioactivity and played a catalytic role in the reduction of H_2O_2 on the surface of modified electrode. Overall, the experimental results established that the multiporous nanofibers of SnO_2 would be an excellent candidate to immobilize biomolecule for constructing a biosensor.

Acknowledgments: This work was supported by Fundamental Research Grant Scheme (RDU140122) and University Malaysia Pahang local researches grant (RDU 140389).

References and Notes

1. A. Turner, I. Karube, and G. S. Wilson, Biosensors: Fundamentals and Applications, Oxford University Press (**1987**).
2. M. Mehrvar and A. Mustafe, *Anal. Sci.* 20, 1113 (**2004**).
3. M. Pohanka and P. Skládal, *J. Appl. Biomed.* 6, 57 (**2008**).
4. S. V. Dzyadevych, V. N. Arkhypova, A. P. Soldatkin, A. V. El'Skaya, C. Martelet, and N. Jaffrezic-Renault, *IRBM* 29, 171 (**2008**).
5. E. Katz, A. F. Bückmann, and I. Willner, *J. Am. Chem. Soc.* 123, 10752 (**2001**).
6. M. Hartmann and X. Kostrov, *Chem. Soc. Rev.* 42, 6277 (**2013**).
7. J. Wang, *Electroanalysis* 13, 983 (**2001**).
8. T. Ahuja, I. A. Mir, and D. Kumar, *Biomaterials* 28, 791 (**2007**).
9. A. Sassolas, L. J. Blum, and B. D. Leca-Bouvier, *Biotechnol. Adv.* 30, 489 (**2012**).
10. Y. Wu and S. Hu, *Microchim. Acta* 159, 1 (**2007**).
11. L. Zhang, G. Han, Y. Liu, J. Tang, and W. Tang, *Sens. Actuators, B: Chemical* 197, 164 (**2014**).
12. C. Chen, Q. Xie, D. Yang, H. Xiao, Y. Fu, Y. Tan, and S. Yao, *RSC Adv.* 3, 4473 (**2013**).
13. A. D. Chowdhury, R. Gangopadhyay, and A. De, *Sens. Actuators, B: Chemical* 190, 348 (**2014**).
14. Y. Liu, J. Gong, W. Wu, Y. Fang, Q. Wang, and H. Gu, *Sens. Actuators, B: Chemical* 222, 588 (**2016**).
15. M. K. Sezgintürk and E. Dinçkaya, *Biosens. Bioelectron.* 23, 1799 (**2008**).
16. Y. Li, H. J. Schluesener, and S. Xu, *Gold Bulletin.* 43, 29 (**2010**).
17. S. K. Arya, P. R. Solanki, M. Datta, and B. D. Malhotra, *Biosens. Bioelectron.* 24, 2810 (**2009**).
18. C. Dhand, M. Das, M. Datta, and B. Malhotra, *Biosens. Bioelectron.* 26, 2811 (**2011**).
19. J. H. Luong, J. D. Glennon, A. Gedanken, and S. K. Vashist, *Microchim. Acta* 184, 369 (**2016**).
20. J. Zhang, B. Yang, Z. Guo, Q. Song, X. Ye, and S. Zheng, *J. Electrochem. Soc.* 164, B3001 (**2017**).
21. A. K. M. Kafi and A. Chen, *Talanta* 79, 97 (**2009**).
22. A. Kafi, N. S. Azmi, M. M. Yusoff, and M. J. Crossley, *J. Nanosci. Nanotechnol.* 17, 5896 (**2017**).
23. P. Das, M. Das, S. R. Chinnadayyala, I. M. Singha, and P. Goswami, *Biosens. Bioelectron.* 79, 386 (**2016**).
24. S. Kumar, W. Ahlawat, R. Kumar, and N. Dilbaghi, *Biosens. Bioelectron.* 70, 498 (**2015**).
25. G.-P. Nikoleli, D. P. Nikolelis, G. Evtugyn, and T. Hianik, *TrAC, Trends Anal. Chem.* 79, 210 (**2016**).
26. M. Gerard, A. Chaubey, and B. Malhotra, *Biosens. Bioelectron.* 17, 345 (**2002**).
27. L. Xia, Z. Wei, and M. Wan, *J. Colloid Interface Sci.* 341, 1 (**2010**).
28. J.-D. Qiu, W.-M. Zhou, J. Guo, R. Wang, and R.-P. Liang, *Anal. Biochem.* 385, 264 (**2009**).
29. A. Chaubey and B. Malhotra, *Biosens. Bioelectron.* 17, 441 (**2002**).
30. F. Patolsky, Y. Weizmann, and I. Willner, *Angew. Chem. Int. Edit.* 43, 2113 (**2004**).
31. A. K. M. Kafi and M. J. Crossley, *Biosens. Bioelectron.* 42, 273 (**2013**).
32. M. A. Kim and W.-Y. Lee, *Anal. Chim. Acta* 479, 143 (**2003**).
33. A. Chen and S. Chatterjee, *Chem. Soc. Rev.* 42, 5425 (**2013**).
34. M. Holzinger, A. Le Goff, and S. Cosnier, *Front. Chem.* 2, 63 (**2014**).
35. E. Singh, M. Meyyappan, and H. S. Nalwa, *ACS Appl. Mater. Interfaces* 9, 34544 (**2017**).
36. R. Singh, E. Singh, and H. S. Nalwa, *RSC Adv.* 7, 48597 (**2017**).
37. S. Pandit, D. Dasgupta, N. Dewan, and P. Ahmed, *J. Pharmacogn. Phytochem.* 5, 104 (**2016**).
38. D. A. Mengistie, M. A. Ibrahem, P.-C. Wang, and C.-W. Chu, *ACS Appl. Mater. Interfaces* 6, 2292 (**2014**).
39. M. Rahman, X.-B. Li, Y.-D. Jeon, H.-J. Lee, S. J. Lee, and J.-J. Lee, *J. Electrochem. Sci. Technol.* 3, 90 (**2012**).
40. A. K. M. Kafi, Qamar Wali, Rajan Jose, Tapan Kumar Biswas, and Mashitah M. Yusoff, *Microchimica Acta* 184, 4443 (**2017**).
41. J. F. Rusling and F. N. Alaa-Eldin, *J. Am. Chem. Soc.* 115, 11891 (**1993**).
42. X. Han, W. Huang, J. Jia, S. Dong, and E. Wang, *Biosens. Bioelectron.* 17, 741 (**2002**).
43. S. Liu, Z. Dai, H. Chen, and H. Ju, *Biosens. Bioelectron.* 19, 963 (**2004**).
44. E. Laviron, *J. Electroanal. Chem. Interfacial Electrochem.* 101, 19 (**1979**).
45. H. Ma, N. Hu, and J. F. Rusling, *Langmuir* 16, 4969 (**2000**).
46. K. Cui, Y. Song, Y. Yao, Z. Huang, and L. Wang, *Electrochem. Commun.* 10, 663 (**2008**).
47. Y. Wang, X. Chen, and J.-J. Zhu, *Electrochem. Commun.* 11, 323 (**2009**).

IP: 5.62.157.167 On: Thu, 06 Dec 2018
Copyright: American Scientific Publishers
Delivered by Ingenta

Received: 30 October 2017. Accepted: 8 December 2017.